Agr. Nat. Resour. 56 (2022) 233–242

AGRICULTURE AND NATURAL RESOURCES

Journal homepage: http://anres.kasetsart.org

Research article

Land cover mapping using Sentinel-2 images in area dominated by small-scale, heterogeneous agricultural parcels

Indarto Indarto*, Chairiyah Umi Rahayu, Siswoyo Soekarno

Department of Agricultural Engineering, Faculty of Agricultural Technology, University of Jember, East Java 68121, Indonesia

Article Info

Article history:
Received 13 July 2021
Revised 18 January 2022
Accepted 28 January 2022
Available online 20 April 2022

Keywords:
Agricultural parcels,
Heterogeneous land,
Land cover,
Sentinel-2,
Small scale

Abstract

Importance of the work: Satellite imagery contains information on a pixel basis and promises an efficient and effective solution for mapping agricultural land resources. However, in tropical regions, the use of medium-resolution optical imagery for land cover (LC) mapping is constrained by the presence of cloud cover, seasonal changes in LC, small agricultural parcels and heterogeneity of patch or landscape features.

Objectives: To analyze and compare the LC classification in a region characterized by small-scale agricultural land occupation.

Materials & Methods: Two scenes of Sentinel-2 images were used. Three well-known pixel-based classification algorithms—maximum likelihood classifier (MLC), extraction and classification of homogeneous objects (ECHO) and the Fisher linear discriminant (FLD)—were investigated and compared. The study covered 3,320.3 km^2 in East Java province, Indonesia.

Results: The classification results produced nine LC classes—pavement or urban area (PUA), heterogeneous agricultural land (HAL), irrigated paddy (IP), open water body (OWB), dense vegetation or forest (DVF), sparse vegetation or plantation (SVP), shrubland or dry-land (SC), wetland (WL) and sand-clay-rock (SCR). Classification using MLC and ECHO produced kappa and overall accuracies of more than 90%. However, classification using the FLD algorithm had lower overall and kappa accuracies of 90.31% and 87.96%, respectively.

Main finding: Of the algorithms, MLC and ECHO were better than FLD. However, four classes (HAL, IP, DVF and SVP) were still difficult to distinguish as the seasonal variation of these four LC classes may propagate different areas based on the different algorithms.

* Corresponding author.
E-mail address: indarto.ftp@unej.ac.id (I. Indarto)

https://doi.org/10.34044/j.anres.2022.56.2.02

Introduction

Up-to-date information about the Earth's surface provided by land cover (LC) maps is essential for numerous environmental and land management applications (Malinowski et al., 2020). The images provided from satellites contain information on a pixel basis and promise an efficient and effective solution for mapping many kinds of phenomena on the Earth's surface.

Sentinel-2 imagery has been applied in many LC classifications (Topaloğlu et al., 2016; Noi and Kappas, 2017; Degife et al., 2018; Ienco et al., 2019; Osgouei et al., 2019; Bolton et al., 2020). Phiri et al. (2020) reported of the many different applications of Sentinel-2 imagery since the satellite was launched in 2015. Chaves et al. (2020) reviewed the comparative use and potential application of the Landsat 8 Operational Land Imager and Sentinel-2 Multispectral Instrument data for acquiring information on landuse and LC.

All image classification and interpretation methods can produce LC thematic maps for a region of interest. However, it is always challenging to compromise between imagery availability (spatial, spectral, temporal resolution) and phenomena to be observed. In addition, the cost-benefit ratio should be considered for imagery and mapping purposes.

Furthermore, classification results may be constrained by a high level of heterogeneity in the landscape. For example, Lu et al. (2004) stated that classification results are greatly influenced by various factors including: the training area, complexity of the landscape, knowledge of the study area, composite bands and processing, classification algorithms and user experience with the classification algorithms. Hence, choosing the appropriate algorithms for image classification may enhance the classification results.

Pixel-based classification, such as the maximum likelihood classifier (MLC), extraction and classification of homogeneous objects (ECHO), and the Fisher linear discriminant (FLD), have been used widely in many remote sensing applications; (Basukala et al., 2017; Noi and Kappas, 2017). A detailed description of MLC can be found in many textbooks (Jensen, 2009; Campbell and Wynne, 2011), where MLC is as a parametric classifier that assumes normal or near-normal spectral distribution for each feature of interest. MLC is based on the probability that a pixel belongs to a particular class. The variability of classes is taken into account by using the covariance matrix. Furthermore, insufficient training samples or multimode distributions often result in poor classification (Lu et al., 2004). MLC has been considered the most common classifier used in practice (Hogland et al., 2013).

The ECHO algorithm was developed by Kettig and Landgrebe (1976) who described it as a multistage, spatial-spectral classifier using elements of a parametric per-pixel classifier and elements related to texture classification. According to Lu et al. (2004), the four stages involved in ECHO classification are: 1) partition of features into cells; 2) setting a user threshold; 3) aggregating cells and individual pixels; and 4) classifying the aggregates of pixels using an MLC to provide final results. The ECHO algorithm has been integrated into the Multispec open-source software (Landgrebe and Biehl, 2011).

Lu et al. (2004) described the FLD as a statistical parametric algorithm based on the homogeneity of pixels and band variance/covariance matrices. Linear discriminant analysis of the training data is implemented to form a set of linear functions and FLD maximizes the variance between classes and minimizes the variance within classes, with the assigned class for each pixel being the class that receives the highest support after evaluating all functions.

More recent image classification development has explored other algorithms (Zhaocong and Deren, 2002) involving for example, semi-automated random forest (Gounaridis et al., 2016), segmentation of image (Basukala et al., 2017; Noi and Kappas, 2017) and object-based (Robertson and King, 2011; Csillik et al., 2019; Liu et al., 2019) Furthermore, machine learning algorithms have become a major component in image classification (Isuhuaylas et al., 2018: Neetu and Ray, 2019; Abdi, 2020).

Lu and Weng (2007) stated that a classification system is designed based on the user's needs, spatial resolution, compatibility with previous work, image-processing and classification algorithms and time constraints. In practice, it is difficult to identify a suitable approach for a given study area, but using a suitable classifier may improve LC classification accuracy (Lu et al., 2004). This study aimed to: 1) map the land cover in a specific area; and 2) compare and evaluate the three most-common pixel-based classification algorithms (MLC, ECHO and FLD) against local landscape heterogeneity.

Materials and Methods

Study site and input data

The study was conducted in the eastern part of East Java province, Indonesia and comprised two regencies and two cities, namely Pasuruan and Probolinggo (Fig. 1), covering 3,320.3 km^2.

Primary input data were Sentinel-2A images of the study area, selected based on minimum cloud cover present. Fig. 1 presents the raw Sentinel-2A images, selected sites for training areas and subset areas. Table 1 shows the metadata of the images used for this study.

The image captured the region of interest on 25 June 2019. The date corresponds to the mid-dry season in most East Java areas; therefore, only minimum cloud cover was present. Consequently, it was the best image available from 2015 to 2019. It is always challenging to obtain optical imagery with minimum cloud coverage in tropical regions.

Procedure

The image processing procedure consisted of pre-treatment, classification and post-treatment (Fig. 2).

The QGIS (QGIS Development Team, 2019) software was used for image pre-treatment. Pre-treatment included atmospheric correction, composite, mosaics and clipping the image using a polygon boundary (Fig.2). First, the Semi-Automatic Classification Plugin (Congedo, 2016), available in QGIS (QGIS Development Team, 2019), was used to process atmospheric correction using the DOS (dark object subtraction) algorithm. Next, four Sentinel bands (bands 2, 3, 4 and 8) were used to make a composite image. Then, the images were visualized using three bands (2, 3 and 4). Finally, the image was clipped using the polygon boundaries of the study areas.

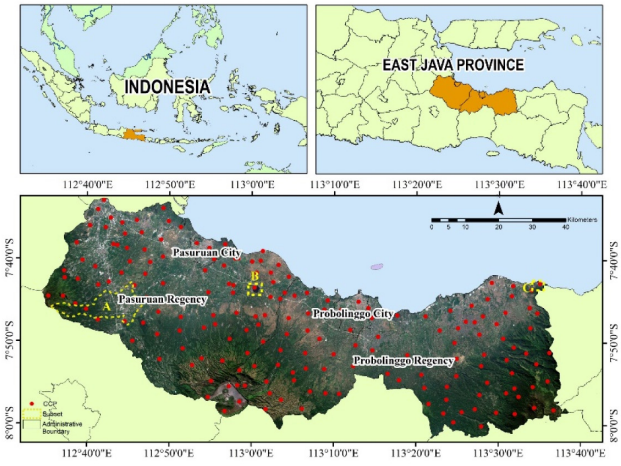

Fig. 1 Study site, Raw Sentinel-2A image, and collected training areas (red points) and subset areas (A and B)

Image classification was processed using Multispec (Landgrebe and Biehl, 2018). Three classification algorithms (MLC, ECHO and FLD) were used for the supervised classification of the pixels (Fig. 2). In this study, Gaussian maximum likelihood was used as an MLC classifier. Then, in the ECHO algorithm, a 2×2 cell was set up as a homogeneous group of pixels. FLD classified pixels using linear likelihood. Furthermore, supervised classification was conducted with the aid of 197 ground control points or training areas. The national standard or SNI 7645:2014 (Badan Standar Nasional, 2014) was applied to determine the number of land cover classes.

Fig. 3 shows the nine selected photos of the field survey representing the land cover classes for the region. A series of field surveys were conducted July–September 2020 and nine primary classes were identified: 1) pavement or urban area (PUA) representing all surface features in urbanized areas, such as housing and industrial sites; 2) heterogeneous agricultural land (HAL) covering all types of agricultural areas not dominated by paddy fields; 3) irrigated paddy (IP) consisting of all areas dominated by paddy, including technically irrigated land; 4) open water body (OWB) representing surface features, such as lakes, rivers and reservoirs; 5) dense vegetation-forest

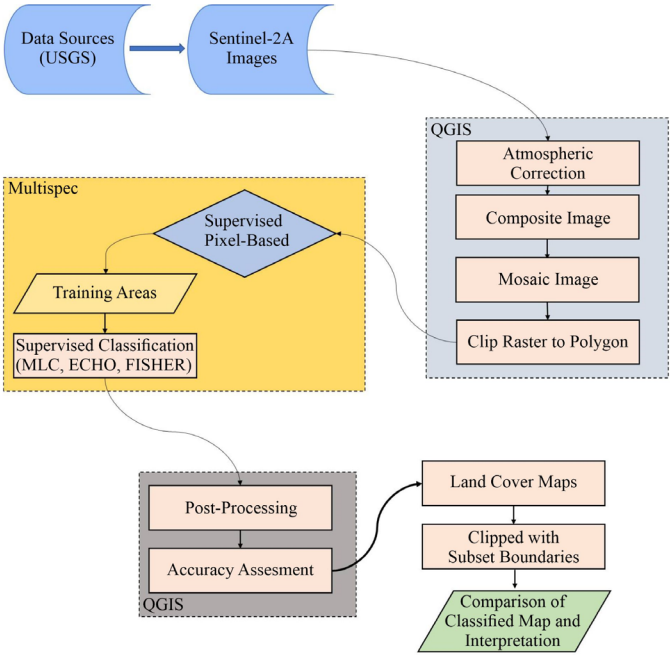

Fig. 2 Image treatment procedure

Table 1 Image metadata

Date acquired	Path/Row	Cloud cover (%)	Data type/Collection category	Orbit
25/06/2019	118/65	0.0179 0.0343	S2A_MSILIC	Descending

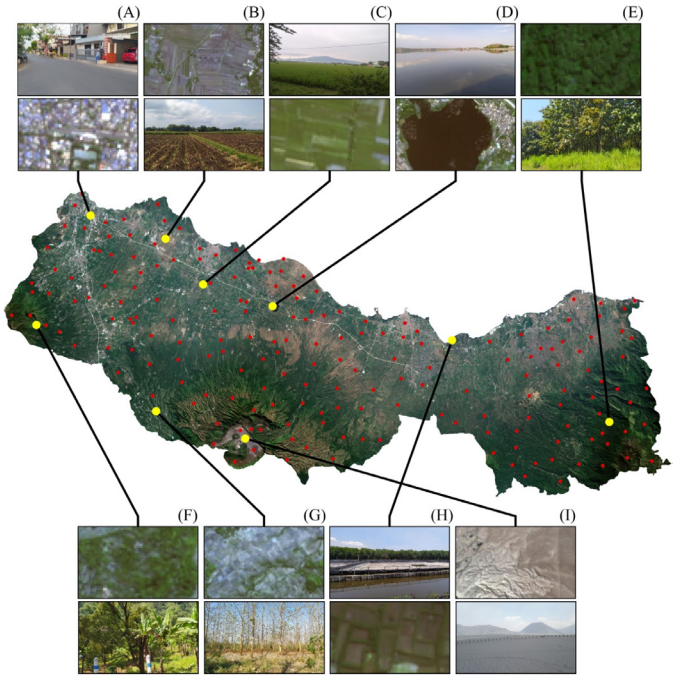

Fig. 3 Images (Fig. 3A–3I) used to visualize land cover classes

(DVF) describing all annual vegetation types: primary tropical forest, secondary forest and mixed plantation; 6) sparse vegetation-plantation (SVP) representing all surface features generally consisting of annual vegetation mixed with seasonal crops; 7) shrubland (SC) including all surface features, such as grass, mixed-grass and dry land with less vegetation or abandoned agricultural land; 8) wetland (WD) showing wet areas dominated by water, where wetland is usually present along sea borders and in East Java, this feature was more dominant in the northern part of the main island; 9) sand/clay/rock (SCR) representing surfaces covered by sand, rock or clay, where sand deposits were also found in other locations and clay and rock represented wasteland or abandoned land.

Table 2 presents a summary of the training areas used that were identified during the field survey. Other training areas were interpreted from Google Earth images.

Two-subset areas were used to compare the classification results. Subset A had a mixture of areas at the district level. Purwosari district (Fig. 4) is located in the hilly areas of

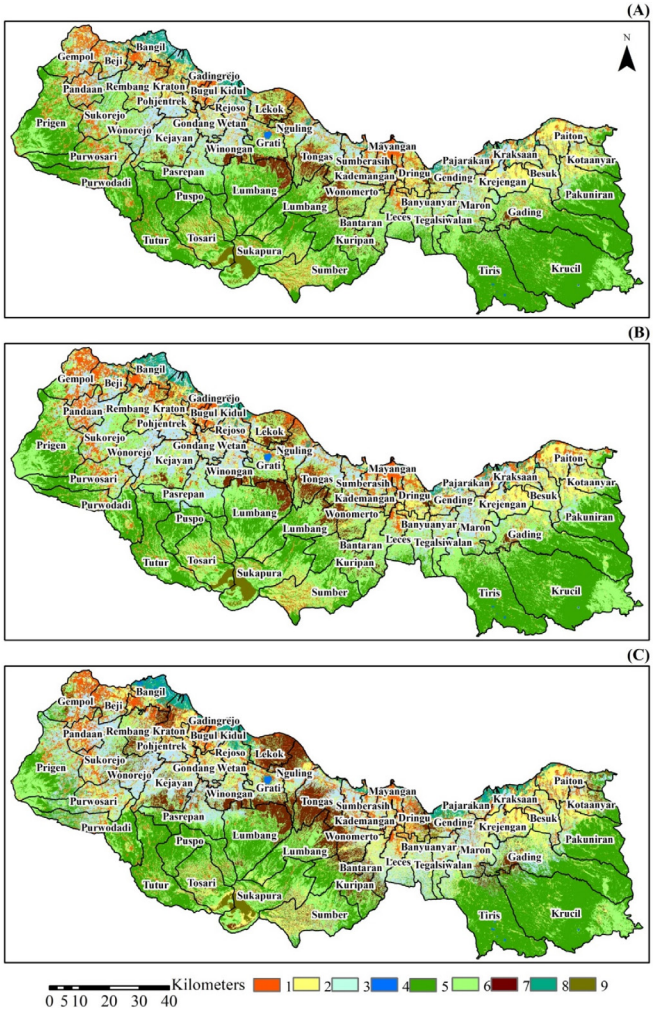

Fig. 4 Classification results of overall study area: (A) maximum likelihood classifier algorithm; (B) extraction and classification of homogeneous objects algorithm; (C) Fisher linear likelihood algorithm, where 1 = pavement or urban area, 2 = heterogeneous agricultural land, 3 = irrigated paddy field, 4 = open water body, 5 = dense vegetation forest, 6 = sparse vegetation plantation, 7 = shrubland, 8 = wetland and 9 = sand-clay-rock

Table 2 Overview of training areas

No	Class	Number of samples	Amount of total area (%)	Area (km²)
1	Pavement or urban area (PUA)	39	7.53	0.06
2	Heterogeneous agricultural (HAL)	34	8.08	0.07
3	Irrigated paddy (IP)	33	18.50	0.16
4	Open water body (OWB)	10	13.95	0.12
5	Dense vegetation-forest (DVF)	30	16.29	0.14
6	Sparse vegetation-plantation (SVP)	15	4.85	0.04
7	Shrubland (SC)	11	6.15	0.05
8	Wetland (WL)	15	2.85	0.02
9	Sand-clay-rock (SCR)	10	21.81	0.18
	Total	197	100.00	0.84

Pasuruan regency. The altitude in Purwosari district was in the range 500–2,000 m above sea level and the terrain slope was in the range 2–45%. The district area contained DVF, SVP, HAL, IP and PUA.

Subset B was a specific area including a small lake (Ranu Grati) that is the only OWB on the Sentinel image. The subset area covered OWB, HAL, PUA and DVF. The raw Sentinel image in subset B was digitized to produce four maps that were used as a control for comparisons of the three maps classified by each algorithm. Finally, the area occupied by each land cover class was calculated and compared.

Results and Discussion

Accuracy assessment

The classification processes produce nine classes of land cover: PUA, HAL, IP, OWB, DVF, SVP, SC, WL and SCR. Tables 3, 4 and 5 present the accuracy assessment resulting from the three algorithms.

The MLC algorithm had an overall accuracy (OA) and kappa accuracy (KA) of 93.28% and 91.61%, respectively (Table 3). Individual accuracy (user accuracy; User Acc.) and reliability accuracy (producer accuracy, Prod Acc.) had values exceeding 85%. The MLC algorithm performed well in this study. Table 4 shows the accuracy assessment for the ECHO algorithm that had OA and KA values of 92.19% and 90.25%, respectively, and User Acc. and Prod. Acc values for each class that exceeded 80%. The FLD algorithm had OA and KA values of 90.31% and 87.96%, respectively (Table 5), with User Acc. Values for each class exceeding 80%, but the Prod Acc. Values for IP and SC were less than < 80%. Thus, the MLC and ECHO algorithms produced better classifications than the FLD algorithm. ECHO classifiers are recommended for tropical land-cover classification, whereas the MLC and FLD algorithms consider per-pixel information and ignore texture or contextual information (Lu et al., 2004). However, in the current study, the MLC algorithm was better than the FLD algorithm because the former is based on the probability that a pixel belongs to a particular class, while the latter minimizes pixel variance within classes, resulting in poor classification in areas dominated by small-scale heterogeneous agriculture that has many pixel variants in several classes.

Land cover of the overall area

Table 6 presents a summary of the areas classified by class. Two algorithms (MLC and ECHO) produced relatively similar area results for six classes (PUA, HAL, OWB, DVF, SC, WL and SCR.

However, the three algorithms (MLC, ECHO, FLD) produced different areas for the classification of IP, DVF and SVP. The mixture of landscapes common in the region may have caused these differences. For example, it was common to find a patch of mixture landscape in the middle of extensive paddy field areas due to housing and backyards, annual vegetation (not actually forested area nor plantation) and seasonal crops. Therefore, using the 10 m ×10 m pixel size, such patches of mixture landscape were still difficult to classify. Controversial results often occur depending on the landscape complexity of the study area and the data used (Lu et al., 2004). Fig. 4 shows the classified land cover maps obtained using the three classification algorithms with thematic map, name and district boundary.

Table 3 Accuracy assessment of maximum likelihood classifier algorithm

Class	User Acc. (%)	PUA	HAL	IP	OWB	DVF	SVP	SC	WL	SCR	Row total
PUA	92.50	74	4	0	0	0	0	2	0	0	80
HAL	95.71	3	67	0	0	0	0	0	0	0	70
IP	94.44	0	0	85	0	0	3	0	2	0	90
OWB	100	0	0	0	10	0	0	0	0	0	10
DVF	95.00	0	0	2	0	190	8	0	0	0	200
SVP	91.33	0	0	10	0	3	137	0	0	0	150
SC	86.67	1	1	0	0	0	0	13	0	0	15
WL	80.00	0	3	0	0	0	0	0	12	0	15
SCR	90.00	1	0	0	0	0	0	0	0	9	10
Column total		79	75	97	10	193	148	15	14	9	640
Producer Acc. (%)		93.67	89.33	87.63	100	98.45	92.57	86.67	85.71	100	

Overall accuracy = 93.28%; Kappa accuracy = 91.61%; Acc. = accuracy

PUA = pavement or urban area; HAL = heterogeneous agricultural; IP = irrigated paddy; OWB = open water body; DVF = dense vegetation-forest; SVP = sparse vegetation-plantation; SC = shrubland; WL = wetland; SCR = sand-clay-rock

Table 4 Accuracy assessment of extraction and classification of homogeneous objects algorithm

Class	User Acc. (%)	PUA	HAL	IP	OWB	DVF	SVP	SC	WL	SCR	Row total
PUA	92.50	74	3	0	0	0	0	3	0	0	80
HAL	97.14	2	68	0	0	0	0	0	0	0	70
IP	94.44	0	0	85	0	0	5	0	0	0	90
OWB	100	0	0	0	10	0	0	0	0	0	10
DVF	94.50	0	0	4	0	189	7	0	0	0	200
SVP	86.67	0	0	15	0	5	130	0	0	0	150
SC	86.67	1	1	0	0	0	0	13	0	0	15
WL	86.67	0	2	0	0	0	0	0	13	0	15
SCR	80.00	2	0	0	0	0	0	0	0	8	10
Column total		79	74	104	10	194	142	16	13	8	640
Producer Acc. (%)		93.67	91.89	81.73	100	97.42	91.55	81	100	100	

Overall accuracy = 92.19%; Kappa accuracy = 90.25%; Acc. = accuracy

PUA = pavement or urban area; HAL = heterogeneous agricultural; IP = irrigated paddy; OWB = open water body; DVF = dense vegetation-forest; SVP = sparse vegetation-plantation; SC = shrubland; WL = wetland; SCR = sand-clay-rock

Table 5 Accuracy assessment of Fisher linear discriminant algorithm

Class	User Acc. (%)	PUA	HAL	IP	OWB	DVF	SVP	SC	WL	SCR	Row total
PUA	90.00	72	5	0	0	0	0	3	0	0	80
HAL	94.29	1	66	0	0	0	0	3	0	0	70
IP	93.33	0	0	84	0	0	6	0	0	0	90
OWB	100.00	0	0	0	10	0	0	0	0	0	10
DVF	88.50	0	0	17	0	177	6	0	0	0	200
SVP	90.00	0	0	12	0	3	135	0	0	0	150
SC	86.67	1	1	0	0	0	0	13	0	0	15
WL	86.67	0	2	0	0	0	0	0	13	0	15
SCR	80.00	2	0	0	0	0	0	0	0	8	10
Column total		76	74	113	10	180	147	19	13	8	640
Producer Acc. (%)		94.74	89.19	74.34	100	98.33	91.84	68	100	100	

Overall accuracy = 90.31%; Kappa accuracy = 87.96%; Acc. = accuracy

PUA = pavement or urban area; HAL = heterogeneous agricultural; IP = irrigated paddy; OWB = open water body; DVF = dense vegetation-forest; SVP = sparse vegetation-plantation; SC = shrubland; WL = wetland; SCR = sand-clay-rock

Table 6 Overall classification results

No	LC	MCL		ECHO		FLD		Average	
	Class	km²	%	km²	%	km²	%	km²	%
1	PUA[1]	337.25	10.16	348.12	10.48	278.30	8.38	321.22	9.67
2	HAL	296.02	8.92	318.20	9.58	460.97	13.88	358.40	10.79
3	IP	382.86	11.53	438.46	13.21	533.12	16.06	451.48	13.60
4	OWB	2.15	0.06	2.12	0.06	8.17	0.25	4.15	0.12
5	DVF	1,056.20	31.81	882.77	26.59	894.40	26.94	944.46	28.45
6	SVP	1,027.36	30.94	1,115.07	33.58	718.34	21.64	953.59	28.72
7	SC	127.61	3.84	128.92	3.88	315.60	9.51	190.71	5.74
8	WL	62.85	1.89	60.44	1.82	77.17	2.32	66.82	2.01
9	SCR	27.97	0.84	26.17	0.79	34.21	1.03	29.45	0.89
	Total	3,320.28	100	3,320.28	100	3,320.28	100	3,320.28	100

LC = Land class; Algorithm types: MLC = maximum likelihood classifier; ECHO = extraction and classification of homogeneous objects; FLD = Fisher linear likelihood

PUA = pavement or urban area; HAL = heterogeneous agricultural; IP = irrigated paddy; OWB = open water body; DVF = dense vegetation-forest; SVP = sparse vegetation-plantation; SC = shrubland; WL = wetland; SCR = sand-clay-rock.

Yellow color = relatively similar area results; grey color = different areas result

In general, using the average values of the three classifications processes (Table 6), PUA occupied about 9.67% of the total area, HAL occupied 10.79%, IP 13.60 % and DVF and SVP combined occupied 57.17%. Both of DVF and SVP represent the landscape features in this region classified as annual vegetation coverage. In reality, the vegetation features present in the field may appear as forest, plantation or a mixed landscape, where the latter may consist of permanent trees, housing and backyard, and seasonal crops. This mixture is automatically classified as either DVF or SPV. The image used for this study was captured during the dry season, where the appearance of these two features is more easily separated from the paddy field feature.

Table 6 shows that the areas of the two classes HAL and SVP were relatively different. Using the MLC algorithm, the sum of these two classes (8.92% + 30.94%) was 39.86%, while using the ECHO algorithm, the cumulative percentage area for these two classes was 43.16% (9.58% + 33.58%), whereas using the FLD algorithm, the sum of these two classes was 35.52% (13.88% + 21.64%). The differences among these values for a class varies depending on the land cover type. The variance within the class affects the results of the classification; the variance within a relatively small class is easier to classify (Lu et al., 2004). The HAL and SPV classes had many pixel variants, resulting in different areas being determined for each algorithm.

Landscape features at district level

Fig. 5 presents a zoomed out result of the classification within Purwosari district. This district is located between major transportation routes connecting the two big cities of East Java (Surabaya in the northwest of the region and Malang in the southwest of the region). The land cover in Purwosari is characterized by a mixed landscape composed of PUA, HAL, IP, DSV and SVP. PUA contains housing, transportation and public facilities.

Tables 6 and 7 show that the FLD algorithm results were not very different from the results using the MLC and ECHO algorithms, while for the last two methods, the classification results were relatively similar.

The greatest differences in the classification results were in the HAL, IP, DVF and SPV classes. The two classes HAL and SPV appear relatively similar in the landscape. Therefore, all three algorithms will classify the pixels in the two classes by considering notable features captured in a pixel or group of pixels. This ambiguity is illustrated by the examples of the two classes in Fig. 6.

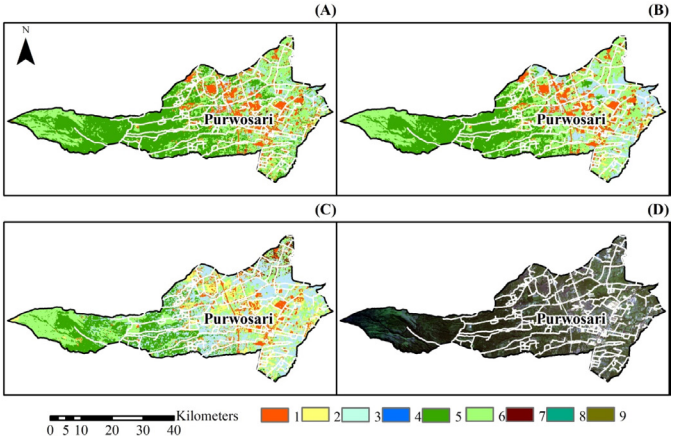

Fig. 5 Visualization of classification results for subset A: (A) maximum likelihood classifier classification result; (B) extraction and classification of homogeneous objects classification result; (C) Fisher linear likelihood classification result; (D) vector layer created from the manual digitalization process; (E) raw Sentinel image as a red/green/blue composite, where 1 = pavement or urban area, 2 = heterogeneous agricultural land, 3 = irrigated paddy field, 4 = open water body, 5 = dense vegetation forest, 6 = sparse vegetation plantation, 7 = shrubland, 8 = wetland and 9 = sand-clay-rock

Table 7 Classification results for subset A

No	Class	MCL		ECHO		FLD		Average	
		km²	%	km²	%	km²	%	km²	%
1	PUA	12.93	16.36	12.15	15.37	9.94	12.57	11.67	14.77
2	HAL	2.98	3.77	4.20	5.31	11.21	14.18	6.13	7.75
3	IP	5.12	6.48	8.71	11.02	22.90	28.97	12.24	15.49
4	OWB	0.002	0.00	0.002	0.00	0.01	0.01	0.00	0.01
5	DVF	30.04	38.00	24.02	30.38	12.60	15.94	22.22	28.11
6	SVP	27.32	34.56	29.41	37.20	21.05	26.63	25.93	32.80
7	SC	0.63	0.80	0.56	0.71	1.30	1.64	0.83	1.05
8	WL	0.00	0.00	0.00	0.00	0.00	0.00	0.00	0.00
9	SCR	0.03	0.04	0.002	0.00	0.04	0.05	0.02	0.03
Total		79.05	100.00	79.05	100.00	79.05	100.00	79.05	100.00

Algorithm types: MLC = maximum likelihood classifier; ECHO = extraction and classification of homogeneous objects; FLD = Fisher linear likelihood PUA = pavement or urban area; HAL = heterogeneous agricultural; IP = irrigated paddy; OWB = open water body; DVF = dense vegetation-forest; SVP = sparse vegetation-plantation; SC = shrubland; WL = wetland; SCR = sand-clay-rock.

Gray color = relatively similar area results.

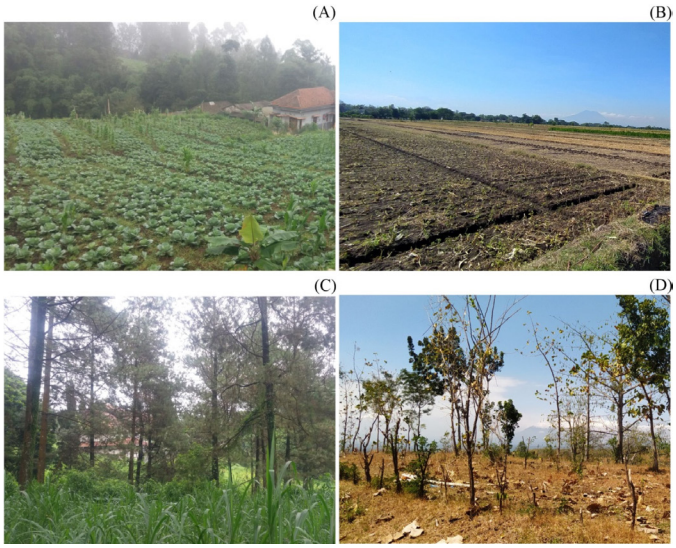

Fig. 6 Mixed landscape classification options for either heterogeneous agricultural land (HAL) or sparse vegetation-plantation (SVP): (A) HAL in mountainous area; (B) HAL in lowland area; (C) SVP in mountainous area; (D) SVP in shared land area

Therefore, features are classified into one class depending on the training area and the majority composition of elements in the landscape. The HAL class is aligned with the concept of landuse, while SVP is more aligned to the concept of land class. The mixture of landscape features present in the field, which may be composed of small-scale heterogeneous agricultural parcels, sparse vegetation and housing, may be classified as HAL or SVP depending on the dominant features in the landscape. The size of landscape features will influence classification and determine the pixel composition captured in Sentinel images.

Comparing features in more detail

Subset B (Fig. 7) visualizes an area of 9.63 km^2 around a water body area known as Lake Grati, which is the only open waterbody in the Sentinel-2A images of the study area. Fig. 7A shows the MLC classification result for this area and Figs. 7B and 7C are taken from the ECHO and FLD classification processes. Fig. 7D is a vector layer created from the manual digitalization process, and Fig. 7E shows the raw Sentinel image as a red/green/blue composite.

Table 8 presents the different classification results obtained using the three algorithms compared to manually digitalizing six classes (HAL, IP, DVF, SVP, WL and SCR). The two MLC and ECHO algorithms produced relatively similar results for three classes (PUA, OWB and SC). The FLD algorithm tended to overestimate PUA, while the ECHO and MLC algorithms produced area results that were relatively similar to manually digitalizing. However, for OWB, the FLD algorithm produced better results compared to the MLC and ECHO algorithms based on the manual estimate. This ambiguity in classification may have resulted from heterogeneity in the landscape, insufficient training samples or the topography of the landscape. The problem can be complicated if medium or coarse spatial resolution data are used for classification because this may result in a large volume of mixed pixels (Lu et al., 2004).

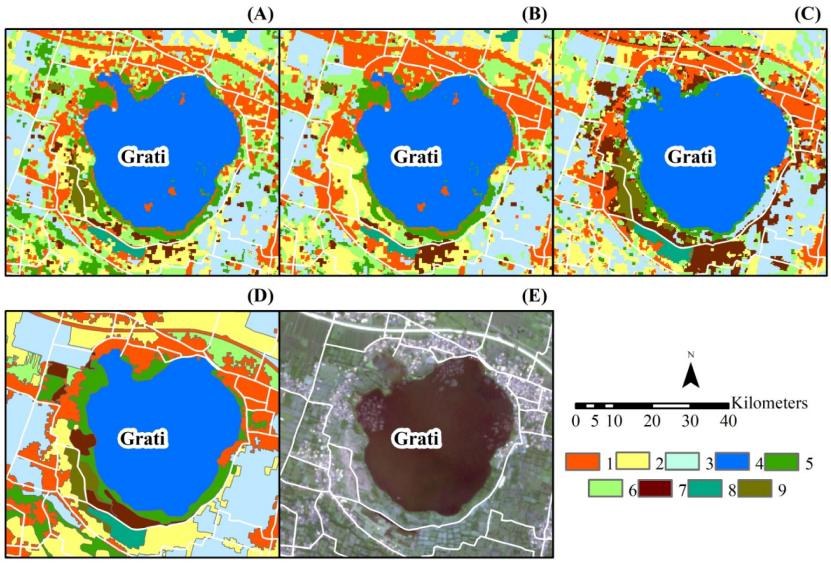

Fig. 7 Visualization of classification results in subset B: (A) maximum likelihood classifier classification result; (B) extraction and classification of homogeneous objects classification result; (C) Fisher linear likelihood classification result; (D) vector layer created from the manual digitalization process; (E) raw Sentinel image as a red/green/blue composite, where 1 = pavement or urban area, 2 = heterogeneous agricultural land, 3 = irrigated paddy field, 4 = open water body, 5 = dense vegetation forest, 6 = sparse vegetation plantation, 7 = shrubland, 8 = wetland and 9 = sand-clay-rock

Table 8 Classification results for subset B

No	Class	MCL		ECHO		FLD		Manual digitialzing		Average	
		km²	%	km²	%	km²	%	km²	%	km²	%
1	PUA[1]	1.35	18.37	1.39	18.91	1.07	14.56	1.48	20.14	1.32	17.99
2	HAL	0.61	8.30	0.95	12.93	1.15	15.65	1.25	17.01	0.99	13.47
3	IP	0.45	6.12	0.67	9.12	0.99	13.47	1.56	21.22	0.92	12,48
4	OWB	1.44	19.59	1.45	19.73	1.61	21.90	1.81	24.63	1.58	21.46
5	DVF	0.44	5.99	0.13	1.77	0.05	0.68	0.59	8.03	0.30	4.12
6	SVP	2.40	32.65	2.22	30.20	1.23	16.73	0.24	3.27	1.52	20.71
7	SC	0.18	2.45	0.17	2.31	0.69	9.39	0.21	2.86	0.31	4.25
8	WL	0.37	5.03	0.35	4.76	0.39	5.31	0.09	1.22	0.30	4.08
9	SCR	0.11	1.50	0.02	0.27	0.17	2.31	0.12	1.63	0.11	1.43
Total		7.35	100.00	7.35	100.00	7.35	100.00	7.35	100.00	7.35	100.00

Algorithm types: MLC = maximum likelihood classifier; ECHO = extraction and classification of homogeneous objects; FLD = Fisher linear likelihood. PUA = pavement or urban area; HAL = heterogeneous agricultural; IP = irrigated paddy; OWB = open water body; DVF = dense vegetation-forest; SVP = sparse vegetation-plantation; SC = shrubland; WL = wetland; SCR = sand-clay-rock

Conclusions

Land cover in the study area (3,320.3 km²) in East Java was mapped using Sentinel-2 images. Two popular algorithms (MLC and ECHO) were applied and compared to the FLD algorithm. The three algorithms were used to classify the major land cover features in the region. The classification processes had overall accuracy (OA) and kappa accuracy (KA) values of 93.28% and 91.61% for the MLC algorithm that were better than for the ECHO algorithm (91.19% and 90.25%, respectively) and the FLD algorithm (90.31% and 87.96%, respectively). Nine major classes were identified: pavement or urban (9.67% average of the three methods); heterogeneous agriculture land (10.79%); irrigated paddy (13.59%); open water body (0.12%); dense vegetation-forest (28.43%); sparse vegetation-plantation (28.70%); shrubland (5.74%); wetland (2.01%); and sand-clay-rock (0.89%). The three algorithms produce different classification results, with the largest differences in three classes (heterogeneous agricultural land, irrigated paddy and sparse vegetation-plantation. These three land cover classes represented the dynamics of land cover that is subject to seasonal change. The spatial resolution of the Sentinel-2 imagery was not adequate to capture the naturally occurring high variability.

Conflict of Interest

The authors declare that there are no conflicts of interest.

Acknowledgments

Publication was supported by a Reworking "Skripsi" Grant from the Research Institute (LP2M), University of Jember, 2020–2021.

References

Abdi, A.M. 2020. Land cover and land use classification performance of machine learning algorithms in a boreal landscape using Sentinel-2 data. Gisci. Remote Sens. 57: 1–20. doi.org/10.1080/15481603.2019.1650447

Basukala, A.K., Oldenburg, C., Schellberg, J., Sultanov, M., Dubovyk, O. 2017. Towards improved land use mapping of irrigated croplands: Performance assessment of different image classification algorithms and approaches. Eur. J. Remote Sens. 50: 187–201. doi.org/10.1080/22797254.2017.1308235

Bolton, D.K., Gray, J.M., Melaas, E.K., Moon, M., Eklundh, L., Friedl, M.A. 2020. Continental-scale land surface phenology from harmonized Landsat 8 and Sentinel-2 imagery. Remote Sens. Environ. 240: 111685. doi.org/10.1016/j.rse.2020.111685

Badan Standar Nasional. 2014. Standar Nasional Indonesia (SNI) 7645:2014 on Land Cover Classification. Jakarta, Indonesia.

Campbell, J.B., Wynne, R.H. 2011. Introduction to Remote Sensing, 5th ed. Guilford Press. New York, NY, USA.

Chaves, M.E.D., Picoli, M.C.A., Sanches, I.D. 2020. Recent applications of Landsat 8/OLI and Sentinel-2/MSI for land use and land cover mapping: A systematic review. Remote Sens. 12: 3062. doi.org/10.3390/rs12183062

Congedo, L. 2017. Semi-automatic classification plugin documentation. https://buildmedia.readthedocs.org/media/pdf/semiautomaticclassificationmanual-v5/latest/semiautomaticclassificationmanual-v5.pdf,

Csillik, O., Belgiu, M., Asner, G.P., Kelly, M. 2019. Object-based time-constrained dynamic time warping classification of crops using Sentinel-2. Remote Sens. 11: 1257. doi.org/10.3390/rs11101257

Degife, A.W., Zabel, F., Mauser, W. 2018. Assessing land use and land cover changes and agricultural farmland expansions in Gambella region, Ethiopia, using Landsat 5 and Sentinel 2a multispectral data. Heliyon 4: e00919. doi.org/10.1016/j.heliyon.2018.e00919

Gounaridis, D., Apostolou, A., Koukoulas, S. 2016. Land cover of Greece, 2010: A semi-automated classification using random forests. J. Maps. 12: 1055–1062. doi.org/10.1080/17445647.2015.1123656

Hogland, J., Billor, N., Anderson, N. 2013. Comparison of standard maximum likelihood classification and polytomous logistic regression used in remote sensing. Eur. J. Remote Sens. 46: 623–640. doi.org/10.5721/EuJRS20134637

Ienco, D., Interdonato, R., Gaetano, R., Minh, D.H.T. 2019. Combining Sentinel-1 and Sentinel-2 satellite image time series for land cover mapping via a multi-source deep learning architecture. ISPRS J. Photogramm. 158: 11–22. doi.org/10.1016/j.isprsjprs.2019.09.016

Isuhuaylas, L.A.V., Hirata, Y., Santos, L.C.V., Torobeo, N.S. 2018. Natural forest mapping in the Andes (Peru): A comparison of the performance of machine-learning algorithms. Remote Sens. 10: 782. doi.org/10.3390/rs10050782

Jensen, J.R. 2009. Remote Sensing of the Environment: An Earth Resource Perspective, 2nd ed. Pearson. London, UK.

Kettig, R.L., Landgrebe, D.A. 1976. Classification of multispectral image data by extraction and classification of homogeneous objects. IEEE T. Geosci. Elect. 14: 19–26. doi.org/10.1109/TGE.1976.294460

Landgrebe, D., Biehl, L. 2018. MultiSpec. Purdue University, West Lafayette, IN, USA. https://engineering.purdue.edu/~biehl/MultiSpec/index.html, 14 June 2019.

Liu, C.C., Zhang, Y.C., Chen, P.Y., Lai, C.C., Chen, Y.H., Cheng, J.H., Ko, M.H. 2019. Clouds classification from Sentinel-2 imagery with deep residual learning and semantic image segmentation. Remote Sens. 11: 119. doi.org/10.3390/rs11020119

Lu, D., Mausel, P., Moran, E., Rudy, J. 2004. Comparison of land-cover classification methods in the Brazilian Amazon basin. Photogramm. Eng. Remote Sens. 70: 723–731. doi.org/10.14358/PERS.70.6.723

Lu, D., Weng, Q. 2007. A survey of image classification methods and techniques for improving classification performance. Int. J. Remote Sens. 28: 823–870. doi.org/10.1080/01431160600746456

Malinowski, R., Lewiński, S., Rybicki, M., et al. 2020. Automated production of a land cover/use map of Europe based on Sentinel-2 imagery. Remote Sens. 12: 3523. doi.org/10.3390/rs12213523

Neetu, Ray, S.S. 2019. Exploring machine learning classification algorithms for crop classification using sentinel 2 data. ISPRS J. Photogramm. Remote Sens. XLII-3/W6: 573–578.

Osgouei, P.E., Kaya, S., Sertel, E., Alganci, U. 2019. Separating built-up areas from bare land in Mediterranean cities using Sentinel-2A imagery. Remote Sens. Environ. 11: 345. doi.org/10.3390/rs11030345

Phiri, D., Simwanda, M., Salekin, S., Nyirenda, V.R., Murayama, Y., Ranagalage, M. 2020. Sentinel-2 data for land cover/use mapping: A review. Remote Sens. Environ. 12: 2291. doi.org/10.3390/rs12142291

QGIS Development Team. 2019. QGIS Geographic Information System. Open Source Geospatial Foundation Project. Zurich, Switzerland. http://qgis.osgeo.org, 5 June 2019.

Robertson, L.D., King, D.J. 2011. Comparison of pixel-and object-based classification in land cover change mapping. Int. J. Remote Sens. 32: 1505–1529. doi.org/10.1080/01431160903571791

Noi, P.T., Kappas, M. 2017. Comparison of random forest, k-nearest neighbor, and support vector machine classifiers for land cover classification using Sentinel-2 imagery. Sensors 18: 18. doi.org/10.3390/s18010018

Topaloğlu, R.H., Sertel, E., Musaoğlu, N. 2016. Assessment of classification accuracies of Sentinel-2 and Landsat-8 data for land cover/use mapping. Int. Arch. Photogramm. Remote Sens. Spatial Inf. Sci. XLI-B8: 1055–1059. doi.org/10.5194/isprs-archives-XLI-B8-1055-2016

Zhaocong, W., Deren, L. 2002. Neural network based on rough sets and its application to remote sensing image classification. Geo-Spat. Inf. Sci. 5: 17–21. doi.org/10.1007/BF02833881